International Journal of Control

ISSN: (Print) (Online) Journal homepage: https://www.tandfonline.com/loi/tcon20

Tracking control for switched nonlinear systems subject to output hysteresis via adaptive multi-dimensional Taylor network approach

Wen-Jing He, Shan-Liang Zhu, Na Li & Yu-Qun Han

INTERNATIONAL JOURNAL OF CONTROL
https://doi.org/10.1080/00207179.2022.2067787

Tracking control for switched nonlinear systems subject to output hysteresis via adaptive multi-dimensional Taylor network approach

Wen-Jing He [a], Shan-Liang Zhu [a,b], Na Li [a] and Yu-Qun Han [a,b]

[a]School of Mathematics and Physics, Qingdao University of Science and Technology, Qingdao, People's Republic of China; [b]The Research Institute for Mathematics and Interdisciplinary Sciences, Qingdao University of Science and Technology, Qingdao, People's Republic of China

ABSTRACT

For switched nonlinear systems with output hysteresis, by working on multi-dimensional Taylor network (MTN), an adaptive control strategy is put forward, which can effectively solve the tracking control problem. Firstly, the modified Bouc–Wen hysteresis model is employed to cope with the nonlinear problem caused by output hysteresis. Secondly, the Nussbaum function is introduced into the control design process, and MTN is used to approach nonlinear structures. Thirdly, a novel network adaptive control strategy is constructed with the help of a common Lyapunov function, which can realize the tracking control and stability of the system simultaneously. It is worth noting that as a new type of neural network, MTN is first used for control of switched systems with output hysteresis. Finally, two simulation examples show that the proposed control strategy is effective.

ARTICLE HISTORY
Received 29 December 2021
Accepted 13 April 2022

KEYWORDS
Adaptive control; multi-dimensional Taylor network; switched nonlinear systems; output hysteresis

1. Introduction

Over the past few decades, for the purpose of solving the issue caused by the nonlinear structures in the control systems, fuzzy logic systems (FLSs) and neural networks (NNs) were extensively used in various systems as two kinds of general-purpose approximate methods (Han et al., 2021; Li et al., 2019a, 2021; Niu et al., 2020; Yue & Li, 2019). It is worth noting that multi-dimensional Taylor network (MTN), as one of NN with a special structure, has attracted quite a lot of attention due to its excellent approximation ability, dynamic performance and simple structure (Yan & Duan, 2021). Many research results of MTN in plenty of systems were published, such as large-scale nonlinear systems (Chu et al., 2021), nonlinear systems (Han, Li et al., 2021), discrete-time nonlinear systems (Duan et al., 2020) and stochastic nonlinear systems (Han, 2018). Nevertheless, there are few research results on MTN for switched nonlinear systems.

In the wake of the rapid developments of automatic control theory, it is not easy to solve the problem faced by control science with a single control model. Consequently, as a kind of unified dynamic mathematical model, the research of hybrid systems has caught extensive attention (Cassandras et al., 2001; Henzinger et al., 1998; Juloski et al., 2005; Zhao et al., 2005). Among them, switched systems, as one of the important hybrid systems, has a wide range of industrial application background (Gong et al., 2011; Min et al., 2021; Zhang et al., 2015). Therefore, the study of switched nonlinear systems has become a research highlight in the field of automation and control, and a host of research achievements have been obtained (Li et al., 2021, 2019b; Mao et al., 2022; Niu et al., 2018). For the control problem of switched nonlinear systems, many control approaches have been proposed, such as decentralized control (Li et al., 2021; Zhang et al., 2021), adaptive control (Wu et al., 2020), robust control (Niu & Zhao, 2012; Xiang et al., 2012), fault-tolerant control (Zou et al., 2021), backstepping design method (Ma & Zhao, 2010; Yin et al., 2020) and so on. Among them, the backstepping design method has received widespread attention since this method can obtain a globally stable controller for the nonlinear systems that do not meet the matching conditions. Subsequently, many adaptive backstepping control strategies have been proposed for quite a lot of important switched nonlinear systems, for instance, uncertain switched systems (Chiang & Fu, 2014; Lai et al., 2018), switched systems with input delay (Niu & Li, 2018) and switched systems without strict feedback (Liu et al., 2017). However, the problem of output hysteresis is not considered in the research achievements mentioned above.

In a multitude of practical systems, the hysteretic phenomenon often occurs, and it seriously degrades the system performance. In view of hysteresis not only depends on the output but also depends on the input, so it is difficult to cope with the hysteresis. In the past period of time, a lot of studies on the hysteresis problem were reported (Chen et al., 2008; Han et al., 2015; Su et al., 2000; Tao & Kokotovic, 1995; Zhou et al., 2012). For systems with hysteresis, authors in Tao and Kokotovic (1995) achieved hysteresis linearisation by

CONTACT Yu-Qun Han yuqunhan@163.com School of Mathematics and Physics, Qingdao University of Science and Technology, Qingdao266061, People's Republic of China; The Research Institute for Mathematics and Interdisciplinary Sciences, Qingdao University of Science and Technology, Qingdao266061, People's Republic of China

constructing hysteresis inverse, which can improve system performance. With the help of the PI model, authors in Chen et al. (2008) proposed an adaptive control strategy for dynamic systems. Authors in Zhou et al. (2012) first proposed a modified Bouc–Wen hysteresis model, which can deal with the control problem of systems subject to more general hysteresis. Since then, the modified Bouc–Wen hysteresis model has become a popular design method to cope with hysteretic problem (Liu et al., 2015; Ma et al., 2019). However, the above methods were mostly focused on general nonlinear systems rather than switched systems, let alone switched nonlinear systems with output hysteresis. Therefore, it is very meaningful to apply the modified Bouc–Wen hysteresis model to switched nonlinear systems with output hysteresis.

On the basis of the above investigations, this article endeavours to develop an adaptive control strategy for a class of switched nonlinear systems with unknown output hysteresis. Firstly, the difficulty caused by the output hysteresis is overcome by introducing the modified Bouc–Wen hysteresis model. Then, in each step of backstepping, the nonlinear structures are approximated by an MTN, and a novel type of network-based adaptive controller is obtained. Finally, the results display that the proposed control strategy is practicable for switched nonlinear systems. The central contributions of this article are as follows:

(1) Although the adaptive MTN backstepping control has achieved some research results for switched nonlinear systems (He et al., 2022; Zhu et al., 2020), the problem of system instability caused by output hysteresis remains unresolved. In addition, although authors in Han (2021) discussed the tracking control issue for systems with output nonlinearity, only the output dead-zone is considered, and the output hysteresis is not considered. Moreover, the proposed MTN-based control strategies in Chu et al. (2021), Han (2021), and Yan and Duan (2021) are not suitable for switched nonlinear systems.

(2) The modified Bouc–Wen hysteresis model proposed in Zhou et al. (2012) is generalised to switched systems for the first time. Unlike the traditional problem of hysteresis for uncertain nonlinear systems (Zhou et al., 2012), this article addresses the issue of output hysteresis for switched nonlinear systems, which is also an important cause of system instability. Although the similar work was studied by Lyu et al. (2019), a novel network controller is structured in this article, which has a simpler structure than that of Lyu et al. (2019).

(3) The control method combining MTN and modified Bouc–Wen hysteresis model is adopted for the first time to settle complex nonlinear problems for switched nonlinear systems subject to output hysteresis, and the amount of calculation can be greatly reduced.

The following notations will be applied in this article. $\boldsymbol{R}^n$ denotes the n-dimensional real space. For a given matrix or vector $\boldsymbol{x}$, $\boldsymbol{x}^{\mathrm{T}}$ means its transpose, $\|\boldsymbol{x}\|$ represents its 2-norm. $\lambda^{\mathrm{T}} P_{m_i}(\boldsymbol{x})$ is defined as MTN with i inputs and intermediate layer polynomials of the highest power m_i.

2. Problem formulation and preliminaries

2.1 System description

The following switched nonlinear systems with unknown output hysteresis are considered.

$$\begin{cases} \dot{\phi}_i = \phi_{i+1} + h_{i,\sigma(t)}\left(\bar{\boldsymbol{\phi}}_i\right) + \Delta_{i,\sigma(t)}\left(t, \bar{\boldsymbol{\phi}}_i\right), \quad 1 \le i \le n-1 \\ \dot{\phi}_n = u + h_{n,\sigma(t)}\left(\bar{\boldsymbol{\phi}}_n\right) + \Delta_{n,\sigma(t)}\left(t, \bar{\boldsymbol{\phi}}_n\right) \\ y = \Gamma\left(\phi_1\right) \end{cases} \tag{1}$$

where $\boldsymbol{\phi} = [\phi_1, \phi_2, \ldots, \phi_n]^{\mathrm{T}} \in \boldsymbol{R}^n$ denotes the state vector, and $\bar{\boldsymbol{\phi}}_i = [\phi_1, \phi_2, \ldots, \phi_i]^{\mathrm{T}} \in \boldsymbol{R}^i$ with $i = 1, 2, \ldots, n$. $\sigma(t) : R_+ \to M = \{1, 2, \ldots, m\}$ denotes the switching signal and m denotes the number of subsystem. For $i = 1, 2, \ldots, n$ and $\forall k \in M$, $h_{i,k}(\bar{\boldsymbol{\phi}}_i)$ represent unknown smooth nonlinear functions and $\Delta_{i,k}(t, \bar{\boldsymbol{\phi}}_i)$ represent the unknown time-varying disturbance. $y = \Gamma(\phi_1)$ represents the output of systems and the hysteresis mechanism. $u(t)$ is the control input.

For reference signal y_d, the main task of this article is to design an adaptive control strategy for system (1) and achieve the following objectives.

(1) For the closed-loop system, all signals in it are bounded;
(2) Tracking error, i.e. $y - y_d$, can converge to an adjustable region of the origin.

Assumption 2.1 (Li et al., 2014): For $\forall t \ge 0$ and $\underline{Y}_0, \bar{Y}_0, Y_1, \ldots, Y_n > 0$ are constants, the y_d and its time derivative $y_d^{(j)}, 1 \le j \le n$ satisfy the inequalities as follows $-\underline{Y}_0 \le y_d(t) \le \bar{Y}_0, |\dot{y}_d(t)| < Y_1, \ldots, |y_d^{(n)}(t)| < Y_n$.

Assumption 2.2: For every $i = 1, 2, \ldots, n$ and $\forall k \in M$, the time-varying disturbance $\Delta_{i,k}(t, \bar{\boldsymbol{\phi}}_i)$ satisfy the following condition.

$$\Delta_{i,k}\left(t, \bar{\boldsymbol{\phi}}_i\right) \le \varphi_{i,k}\left(t, \bar{\boldsymbol{\phi}}_i\right) + \tilde{\varphi}_{i,k} \tag{2}$$

where $\varphi_{i,k}(t, \bar{\boldsymbol{\phi}}_i)$ are unknown functions and $\tilde{\varphi}_{i,k}$ are unknown constants.

Remark 2.1: The main idea of (2) comes from Liu et al. (2015). A more general form of expansion and contraction for the time-varying disturbance is taken into account in this article.

2.2 Processing of output item

The output hysteresis problem is solved by the modified Bouc–Wen hysteresis model, which was reported in Zhou et al. (2012). Its mathematical model is as follows

$$y = \Gamma\left(\phi_1\right) = \rho_1 \phi_1 + \rho_2 \hbar \tag{3}$$

where ρ_1, ρ_2 are unknown constants and satisfy $sign(\rho_1) = sign(\rho_2)$. $\hbar$ is an auxiliary variable, which can be solved by the following differential equation.

$$\begin{cases} \dot{\hbar} & = \dot{\phi}_1 - \iota \left|\dot{\phi}_1\right| |\hbar|^{K-1} \hbar - \varpi \dot{\phi}_1 |\hbar|^K = \dot{\phi}_1 h\left(\hbar, \dot{\phi}_1\right) \\ \hbar_0 & = 0 \end{cases} \tag{4}$$

where ι, ϖ, K are hysteretic parameters and satisfy conditions $\iota > |\varpi|, K > 1$.

$$h\left(\hbar, \dot{\phi}_1\right) = 1 - sign\left(\dot{\phi}_1\right) \iota |\hbar|^{K-1} \hbar - \varpi |\hbar|^K \tag{5}$$

Then, the inverse of model (3) can be expressed as

$$\phi_1 = \Gamma^{-1}(y) = \frac{1}{\rho_1} y - \frac{\rho_2}{\rho_1} \hbar_1 \tag{6}$$

where $\dot{\hbar}_1 = \frac{1}{\rho_2 h(\hbar_1, \frac{\dot{y}}{\rho_1}) + \rho_1} \dot{y} h(\hbar_1, \frac{\dot{y}}{\rho_1})$ and $h(\hbar_1, \frac{\dot{y}}{\rho_1})$ can be defined by (5).

The variable $\kappa(t)$ is defined as follows

$$\kappa(t) = \rho_1 + \rho_2 h\left(\hbar, \dot{\phi}_1\right) \tag{7}$$

So it can be concluded that $\dot{y} = \kappa(t)\dot{\phi}_1$.

Assumption 2.3 (Liu et al., 2015)**:** The value range $\kappa(t)$ is $[-\bar{\kappa}, -\underline{\kappa}] \cup [\underline{\kappa}, \bar{\kappa}]$. Among them, positive constants $\underline{\kappa}, \bar{\kappa}$ are defined as

$$\begin{aligned} \underline{\kappa} &= |\rho_1| \\ \bar{\kappa} &= |\rho_1| + |\rho_2| \left(1 + \frac{\iota}{\iota + \varpi} + \frac{|\varpi|}{\iota + \varpi}\right) \end{aligned} \tag{8}$$

2.3 Nussbaum-Type function

Definition 2.1 (Liu et al., 2015)**:** For variable ε, if the following conditions are satisfied, the function $N(\varsigma)$ is said to be a Nussbaum function.

$$\begin{aligned} \lim_{\varepsilon \to \pm\infty} \sup \frac{1}{\varepsilon} \int_0^{\varepsilon} N(\varsigma)\, d\varsigma &= \infty \\ \lim_{\varepsilon \to \pm\infty} \inf \frac{1}{\varepsilon} \int_0^{\varepsilon} N(\varsigma)\, d\varsigma &= -\infty \end{aligned} \tag{9}$$

It should be pointed out that many functions satisfy the condition of (9), such as $\varsigma^2 \cos\varsigma, \varsigma^2 \sin\varsigma, \exp(\varsigma^2)$. For the Nussbaum function, the following Lemma holds.

Lemma 2.1 (Zhang & Ge, 2007)**:** *Supposing* $\Psi(t)$ *and* $\varsigma(t)$ *are smooth functions defined in* $[0, t_f]$. *Then* $\Psi(t)$, $\varsigma(t)$, $\int_0^{t_f} (\Xi(t)N(\varsigma) + 1)\dot{\varsigma} e^{-\Theta_2(t-\tau)} d\tau$ *are all bounded for* $t \in [0, t_f]$ *and* $t_f < +\infty$, *if the following inequality holds*

$$0 \le \Psi(t) \le \Theta_1 + \int_0^{t_f} (\Xi(t) N(\varsigma) + 1)\, \dot{\varsigma} e^{-\Theta_2(t-\tau)}\, d\tau \tag{10}$$

where $\Xi(t)$ *is the time-varying coefficient with value on* $\mathrm{E} := [\Upsilon^-, \Upsilon^+]$ *and* $0 \notin \mathrm{E}$. $N(\varsigma)$ *is a smooth Nussbaum-type function.* Θ_1, Θ_2 *are positive scalars.* τ *is a variable.*

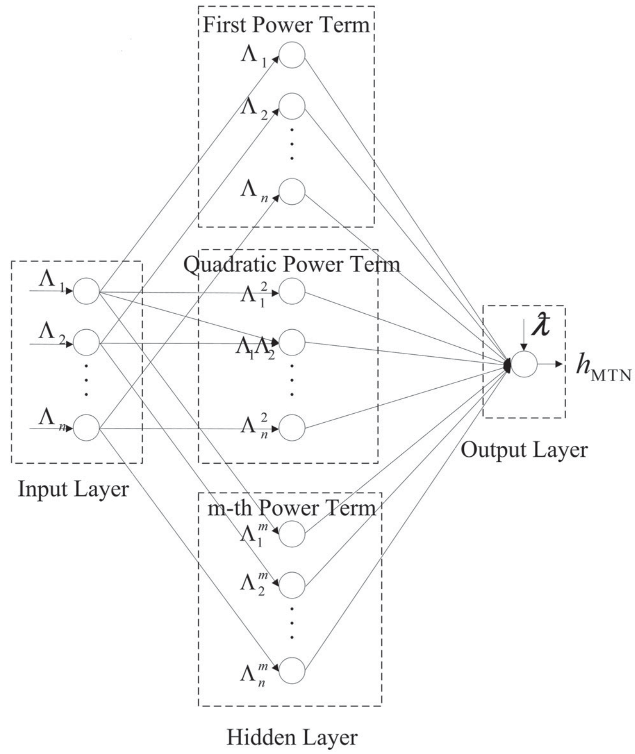

Figure 1. MTN's structure.

2.4 Multi-dimensional Taylor network

MTN is an especially three layer NN, and its structure is shown in Figure 1. In this article, an MTN is introduced into the controller design process to handle with unknown nonlinearity. For MTN, the following Lemma holds

Lemma 2.2 (Han, 2021)**:** *On a compact set* Ω, *for a continuous function* $h(\mathbf{\Lambda}) : \boldsymbol{R}^n \to \boldsymbol{R}$, *and* $\forall \beta > 0$, *there exists an MTN* $\lambda^{\mathrm{T}} P_{m_n}(\mathbf{\Lambda})$ *as follows*

$$h(\mathbf{\Lambda}) = \lambda^{*\mathrm{T}} P_{m_n}(\mathbf{\Lambda}) + \delta(\mathbf{\Lambda}) \tag{11}$$

with $P_{m_n}(\mathbf{\Lambda}) \triangleq \left[\Lambda_1, \cdots, \Lambda_n, \Lambda_1^2, \cdots, \Lambda_n^2, \cdots, \Lambda_1^m, \cdots, \Lambda_n^m\right]^{\mathrm{T}} \in \boldsymbol{R}^l$ *is the middle layer vector of MTN.* $\mathbf{\Lambda} \triangleq [\Lambda_1, \Lambda_2, \cdots, \Lambda_n]^{\mathrm{T}} \in \boldsymbol{R}^n$ *is the input vector of MTN.* $\delta(\mathbf{\Lambda})$ *is the approximate error between* $h(\mathbf{\Lambda})$ *and* $\lambda^{\mathrm{T}} P_{m_n}(\mathbf{\Lambda})$, *and* $|\delta(\mathbf{\Lambda})| < \beta$. λ *is the weight vector of MTN, and*

$$\lambda^* := \arg\min_{\lambda \in \boldsymbol{R}^l} \left\{ \sup_{\Lambda \in \Omega} \left| h(\mathbf{\Lambda}) - \lambda^{\mathrm{T}} P_{m_n}(\mathbf{\Lambda}) \right| \right\} \in \boldsymbol{R}^l.$$

3. Adaptive MTN tracking controller design

First of all, unknown constants $\lambda_i = \max\{\| \lambda_{i,k}\|^2 : k \in M, i = 1, 2, \ldots, n\}$ are defined. $\lambda_{i,k}$ are weight vectors of MTN, and its value will be given later. $\hat{\lambda}_i$ are estimated value of λ_i and satisfy $\tilde{\lambda}_i = \lambda_i - \hat{\lambda}_i$.

Secondly, the coordinate transformation is defined as follows

$$\begin{cases} q_1 & = y - y_d \\ q_i & = \phi_i - \xi_{i-1}, i = 2, \ldots, n \end{cases} \tag{12}$$

where y_d is the reference signal. $\xi_i (i = 1, \ldots, n-1)$ are virtual control signals, which value will be given in later design.

Step 1 : The candidate Lyapunov function is considered as follows

$$\Psi_1 = \frac{1}{2}q_1^2 + \frac{1}{2}\tilde{\lambda}_1^2 \tag{13}$$

The time differentiation of Ψ_1 can be expressed as

$$\dot{\Psi}_1 = q_1\kappa(t)\left(q_2 + \xi_1 + h_{1,k}\left(\bar{\boldsymbol{\phi}}_1\right) + \Delta_{1,k}\left(t, \bar{\boldsymbol{\phi}}_1\right)\right) - q_1\dot{y}_d - \tilde{\lambda}_1\dot{\hat{\lambda}}_1 \tag{14}$$

With the help of Young's inequality and Assumption 2.2, the following inequalities can be obtained.

$$\kappa(t)\, q_1 q_2 \le \frac{1}{2}q_1^2 + \frac{1}{2}\bar{\kappa}^2 q_2^2 \tag{15}$$

$$\kappa(t)\, q_1\left(h_{1,k}\left(\bar{\boldsymbol{\phi}}_1\right) + \Delta_{1,k}\left(t, \bar{\boldsymbol{\phi}}_1\right)\right) \le \frac{1}{2}a_1^2 + \frac{\bar{\kappa}^2}{2a_1^2}q_1^2\gamma_{1,k}^2 \tag{16}$$

with $\gamma_{1,k} = h_{1,k}(\bar{\boldsymbol{\phi}}_1) + \varphi_{1,k}(t, \bar{\boldsymbol{\phi}}_1) + \tilde{\varphi}_{1,k}$, and $a_1 > 0$ is a constant.

Substituting (15) and (16) into (14), the following inequality holds

$$\dot{\Psi}_1 \le \frac{1}{2}q_1^2 + \frac{\bar{\kappa}^2}{2}q_2^2 + \kappa(t)\, q_1\xi_1 + \frac{1}{2}a_1^2 + q_1\mathrm{H}_{1,k} - (2w_1 + 1)\, q_1^2 - \tilde{\lambda}_1\dot{\hat{\lambda}}_1 \tag{17}$$

where $\mathrm{H}_{1,k} = \frac{\bar{\kappa}^2}{2a_1^2}q_1\gamma_{1,k}^2 - \dot{y}_d + (2w_1+1)q_1$ is an unknown function, and $w_1 > 0$ is a constant. According to Lemma 2.2, for $\forall\beta_{1,k} > 0$, exist an MTN that can be used to approximate $\mathrm{H}_{1,k}$, such as

$$\mathrm{H}_{1,k} = \boldsymbol{\lambda}_{1,k}^{\mathrm{T}} P_{m_1}\left(\boldsymbol{q}_1\right) + \delta_{1,k}\left(\boldsymbol{q}_1\right), \left|\delta_{1,k}\left(\boldsymbol{q}_1\right)\right| \le \beta_{1,k} \tag{18}$$

with $\boldsymbol{q}_1 = [q_1]^{\mathrm{T}}$. $\delta_{1,k}(\boldsymbol{q}_1)$ is the error between $\mathrm{H}_{1,k}$ and $\boldsymbol{\lambda}_{1,k}^{\mathrm{T}} P_{m_1}(\boldsymbol{q}_1)$.

With the help of (18) and Young's inequality, the following inequality is true.

$$\begin{aligned} q_1\mathrm{H}_{1,k} &= q_1\boldsymbol{\lambda}_{1,k}^{\mathrm{T}} P_{m_1} + q_1\delta_{1,k} \\ &\le \frac{1}{2}\ell_1^2 + \frac{1}{2\ell_1^2}q_1^2\left\|\boldsymbol{\lambda}_{1,k}\right\|^2 P_{m_1}^{\mathrm{T}} P_{m_1} + \frac{1}{2}q_1^2 + \frac{1}{2}\beta_{1,k}^2 \\ &\le \frac{1}{2}\ell_1^2 + \frac{1}{2\ell_1^2}q_1^2\lambda_1 P_{m_1}^{\mathrm{T}} P_{m_1} + \frac{1}{2}q_1^2 + \frac{1}{2}\beta_{1,k}^2 \end{aligned} \tag{19}$$

where $\ell_1 > 0$ denotes a constant.

Then, the intermediate control signal ξ_1 is designed as follows

$$\xi_1 = N(\varsigma)\left[-\left(w_1 + \frac{1}{2}\right)q_1 + \frac{1}{2\ell_1^2}q_1\hat{\lambda}_1 P_{m_1}^{\mathrm{T}} P_{m_1}\right] \tag{20}$$

Combining (17), (19) and (20), one has

$$\dot{\Psi}_1 \le -\left(w_1 - \frac{1}{2}\right)q_1^2 + \frac{\bar{\kappa}^2}{2}q_2^2 + \left[\kappa(t)\, N(\varsigma) + 1\right]\dot{\varsigma} + \tilde{\lambda}_1\left(\frac{1}{2\ell_1^2}q_1^2 P_{m_1}^{\mathrm{T}} P_{m_1} - \dot{\hat{\lambda}}_1\right) + \frac{1}{2}a_1^2 + \frac{1}{2}\ell_1^2 + \frac{1}{2}\beta_{1,k}^2 \tag{21}$$

where adaptive law $\dot{\varsigma} = -(w_1 + \frac{1}{2})q_1^2 + \frac{1}{2\ell_1^2}q_1^2\hat{\lambda}_1 P_{m_1}^{\mathrm{T}} P_{m_1}$.

Remark 3.1: Term $\frac{\bar{\kappa}^2}{2}q_2^2$ will be solved in the *Step* 2.

Step 2: The candidate Lyapunov function is considered as follows

$$\Psi_2 = \Psi_1 + \frac{1}{2}q_2^2 + \frac{1}{2}\tilde{\lambda}_2^2 \tag{22}$$

The expression for the time derivative of Ψ_2 is shown below

$$\dot{\Psi}_2 = q_2\left(q_3 + \xi_2 + h_{2,k}\left(\bar{\boldsymbol{\phi}}_2\right) + \Delta_{2,k}\left(t, \bar{\boldsymbol{\phi}}_2\right)\right) - q_2\dot{\xi}_1 - \tilde{\lambda}_2\dot{\hat{\lambda}}_2 + \dot{\Psi}_1 \tag{23}$$

where

$$\dot{\xi}_1 = \frac{\partial\xi_1}{\partial y}\dot{y} + \sum_{j=0}^{1}\frac{\partial\xi_1}{\partial y_d^{(j)}}y_d^{(j+1)} + \frac{\partial\xi_1}{\partial\phi_1}\dot{\phi}_1 + \frac{\partial\xi_1}{\partial\varsigma}\dot{\varsigma} + \frac{\partial\xi_1}{\partial\hat{\lambda}_1}\dot{\hat{\lambda}}_1.$$

With the help of Young's inequality, the following inequalities can be obtained.

$$\begin{aligned} -q_2\dot{\xi}_1 \le{}& \frac{1}{4}a_1^2 + \frac{1}{a_1^2}q_2^2\left(\frac{\partial\xi_1}{\partial y}\right)^2\bar{\kappa}^2\left(\phi_2 + \gamma_{1,k}\right)^2 \\ &- q_2\sum_{j=0}^{1}\frac{\partial\xi_1}{\partial y_d^{(j)}}y_d^{(j+1)} - q_2\frac{\partial\xi_1}{\partial\varsigma}\dot{\varsigma} - q_2\frac{\partial\xi_1}{\partial\hat{\lambda}_1}\dot{\hat{\lambda}}_1 + \frac{1}{4}a_1^2 \\ &+ \frac{1}{a_1^2}q_2^2\left(\frac{\partial\xi_1}{\partial\phi_1}\right)^2\left(\phi_2 + \gamma_{1,k}\right)^2 \end{aligned} \tag{24}$$

$$q_2 q_3 \le \frac{1}{2}q_2^2 + \frac{1}{2}q_3^2 \tag{25}$$

$$q_2\left(h_{2,k}\left(\bar{\boldsymbol{\phi}}_2\right) + \Delta_{2,k}\left(t, \bar{\boldsymbol{\phi}}_2\right)\right) \le a_2^2 + \frac{1}{4a_2^2}q_2^2\gamma_{2,k}^2 \tag{26}$$

with $\gamma_{2,k} = h_{2,k}(\bar{\boldsymbol{\phi}}_2) + \varphi_{2,k}(t, \bar{\boldsymbol{\phi}}_2) + \tilde{\varphi}_{2,k}$, and $a_2 > 0$ is a constant.

Substituting (24), (25) and (26) into (23), the following inequality holds

$$\dot{\Psi}_2 \le \dot{\Psi}_1 + \frac{1}{2}q_2^2 + \frac{1}{2}q_3^2 + q_2\xi_2 + a_2^2 + \frac{1}{2}a_1^2 + q_2\mathrm{H}_{2,k} - \frac{\bar{\kappa}^2}{2}q_2^2 - \tilde{\lambda}_2\dot{\hat{\lambda}}_2 \tag{27}$$

where

$$\begin{aligned} \mathrm{H}_{2,k} ={}& \frac{1}{4a_2^2}q_2\gamma_{2,k}^2 + \frac{1}{a_1^2}q_2\left(\frac{\partial\xi_1}{\partial y}\right)^2\bar{\kappa}^2(\phi_2 + \gamma_{1,k})^2 \\ &- \sum_{j=0}^{1}\frac{\partial\xi_1}{\partial y_d^{(j)}}y_d^{(j+1)} - \frac{\partial\xi_1}{\partial\varsigma}\dot{\varsigma} - \frac{\partial\xi_1}{\partial\hat{\lambda}_1}\dot{\hat{\lambda}}_1 \\ &+ \frac{\bar{\kappa}^2}{2}q_2 + \frac{1}{a_1^2}q_2(\frac{\partial\xi_1}{\partial\phi_1})^2(\phi_2 + \gamma_{1,k})^2. \end{aligned}$$

According to Lemma 2.2, for $\forall\beta_{2,k} > 0$, exist an MTN that can be used to approximate $\mathrm{H}_{2,k}$, such as

$$\mathrm{H}_{2,k} = \boldsymbol{\lambda}_{2,k}^{\mathrm{T}} P_{m_2} + \delta_{2,k}\left(\boldsymbol{q}_2\right), \left|\delta_{2,k}\left(\boldsymbol{q}_2\right)\right| \le \beta_{2,k} \tag{28}$$

with $\boldsymbol{q}_2 = [q_1, q_2]^{\mathrm{T}}$. $\delta_{2,k}(\boldsymbol{q}_2)$ is the error between $\mathrm{H}_{2,k}$ and $\boldsymbol{\lambda}_{2,k}^{\mathrm{T}} P_{m_2}$.

From (28) and Young's inequality, one has

$$q_2\mathrm{H}_{2,k} = q_2\,\boldsymbol{\lambda}_{2,k}^{\mathrm{T}} P_{m_2} + q_2\delta_{2,k} \le \frac{1}{2}\ell_2^2 + \frac{1}{2\ell_2^2}q_2^2\,\|\boldsymbol{\lambda}_{2,k}\|^2\,P_{m_2}^{\mathrm{T}}P_{m_2} + \frac{1}{2}q_2^2 + \frac{1}{2}\beta_{2,k}^2 \le \frac{1}{2}\ell_2^2 + \frac{1}{2\ell_2^2}q_2^2\lambda_2 P_{m_2}^{\mathrm{T}}P_{m_2} + \frac{1}{2}q_2^2 + \frac{1}{2}\beta_{2,k}^2 \tag{29}$$

where $\ell_2 > 0$ is a constant.

Then, the intermediate control signal ξ_2 is designed as follows

$$\xi_2 = -\left(w_2 + \frac{1}{2}\right)q_2 - \frac{1}{2\ell_2^2}q_2\,\hat{\lambda}_2 P_{m_2}^{\mathrm{T}}P_{m_2} \tag{30}$$

where $w_2 > 0$ is a constant.

Combining (21), (27), (29) and (30), one has

$$\dot{\Psi}_2 \le -\sum_{j=1}^{2} c_j q_j^2 + \frac{1}{2}q_3^2 + [\kappa(t)N(\varsigma)+1]\,\dot{\varsigma} + \sum_{j=1}^{2}\tilde{\lambda}_j\left(\frac{1}{2\ell_j^2}q_j^2P_{m_j}^{\mathrm{T}}P_{m_j} - \dot{\hat{\lambda}}_j\right) + \sum_{j=1}^{2}a_j^2 + \frac{1}{2}\sum_{j=1}^{2}\ell_j^2 + \frac{1}{2}\sum_{j=1}^{2}\beta_{j,k}^2 \tag{31}$$

where for $i = 1, 2, \ldots, n$, $c_i = w_i - \frac{1}{2}$ are constants.

Step 3: The candidate Lyapunov function is considered as follows

$$\Psi_3 = \Psi_2 + \frac{1}{2}q_3^2 + \frac{1}{2}\tilde{\lambda}_3^2 \tag{32}$$

The time derivative of Ψ_3 has the form displayed below

$$\dot{\Psi}_3 = q_3\left(q_4 + \xi_3 + h_{3,k}\left(\bar{\boldsymbol{\phi}}_3\right) + \Delta_{3,k}\left(t,\bar{\boldsymbol{\phi}}_3\right)\right) - q_3\dot{\xi}_2 - \tilde{\lambda}_3\dot{\hat{\lambda}}_3 + \dot{\Psi}_2 \tag{33}$$

where $\dot{\xi}_2 = \frac{\partial\xi_2}{\partial y}\dot{y} + \sum_{j=0}^{2}\frac{\partial\xi_2}{\partial y_d^{(j)}}y_d^{(j+1)} + \sum_{j=1}^{2}\frac{\partial\xi_2}{\partial\phi_j}\dot{\phi}_j + \frac{\partial\xi_2}{\partial\varsigma}\dot{\varsigma} + \sum_{j=1}^{2}\frac{\partial\xi_2}{\partial\hat{\lambda}_j}\dot{\hat{\lambda}}_j$.

With the help of Young's inequality, the following inequalities can be obtained.

$$-q_3\dot{\xi}_2 \le \frac{1}{4}a_2^2 - q_3\sum_{j=0}^{2}\frac{\partial\xi_2}{\partial y_d^{(j)}}y_d^{(j+1)} - q_3\sum_{j=1}^{2}\frac{\partial\xi_2}{\partial\hat{\lambda}_j}\dot{\hat{\lambda}}_j + \frac{1}{4}a_2^2 - q_3\frac{\partial\xi_2}{\partial\varsigma}\dot{\varsigma} + \frac{1}{a_2^2}q_3^2\sum_{j=1}^{2}\left(\frac{\partial\xi_2}{\partial\phi_j}\right)^2(\phi_{j+1}+\gamma_{j,k})^2 + \frac{1}{a_2^2}q_3^2\left(\frac{\partial\xi_2}{\partial y}\right)^2\bar{\kappa}^2(\phi_2+\gamma_{1,k})^2 \tag{34}$$

$$q_3q_4 \le \frac{1}{2}q_3^2 + \frac{1}{2}q_4^2 \tag{35}$$

$$q_3\left(h_{3,k}\left(\bar{\boldsymbol{\phi}}_3\right) + \Delta_{3,k}\left(t,\bar{\boldsymbol{\phi}}_3\right)\right) \le a_3^2 + \frac{1}{4a_3^2}q_3^2\gamma_{3,k}^2 \tag{36}$$

where $\gamma_{3,k} = h_{3,k}(\bar{\boldsymbol{\phi}}_3) + \varphi_{3,k}(t,\bar{\boldsymbol{\phi}}_3) + \tilde{\varphi}_{3,k}$, and $a_3 > 0$ is a constant.

Substituting (34), (35) and (36) into (33), the following inequality holds

$$\dot{\Psi}_3 \le \dot{\Psi}_2 + \frac{1}{2}q_3^2 + \frac{1}{2}q_4^2 + q_3\xi_3 + a_3^2 + \frac{1}{2}a_2^2 + q_3\mathrm{H}_{3,k} - \frac{1}{2}q_3^2 - \tilde{\lambda}_3\dot{\hat{\lambda}}_3 \tag{37}$$

where

$$\mathrm{H}_{3,k} = \frac{1}{4a_3^2}q_3\gamma_{3,k}^2 + \frac{1}{a_2^2}q_3\left(\frac{\partial\xi_2}{\partial y}\right)^2\bar{\kappa}^2(\phi_2+\gamma_{1,k})^2 - \sum_{j=0}^{2}\frac{\partial\xi_2}{\partial y_d^{(j)}}y_d^{(j+1)} - \frac{\partial\xi_2}{\partial\varsigma}\dot{\varsigma} - \sum_{j=1}^{2}\frac{\partial\xi_2}{\partial\hat{\lambda}_j}\dot{\hat{\lambda}}_j + \frac{1}{2}q_3 + \frac{1}{a_2^2}q_3\sum_{j=1}^{2}\left(\frac{\partial\xi_2}{\partial\phi_j}\right)^2(\phi_{j+1}+\gamma_{j,k})^2.$$

According to Lemma 2.2, for $\forall\beta_{3,k} > 0$, exist an MTN that can be used to approximate $\mathrm{H}_{3,k}$, such as

$$\mathrm{H}_{3,k} = \boldsymbol{\lambda}_{3,k}^{\mathrm{T}}P_{m_3} + \delta_{3,k}(\boldsymbol{q}_3),\ |\delta_{3,k}(\boldsymbol{q}_3)| \le \beta_{3,k} \tag{38}$$

with $\boldsymbol{q}_3 = [q_1, q_2, q_3]^{\mathrm{T}}$. $\delta_{3,k}(\boldsymbol{q}_3)$ is the error between $\mathrm{H}_{3,k}$ and $\lambda_{3,k}^{\mathrm{T}}P_{m_3}$.

From (38) and Young's inequality, the following inequality holds

$$q_3\mathrm{H}_{3,k} = q_3\,\lambda_{3,k}^{\mathrm{T}}P_{m_3} + q_3\delta_{3,k} \le \frac{1}{2}\ell_3^2 + \frac{1}{2\ell_3^2}q_3^2\,\|\lambda_{3,k}\|^2\,P_{m_3}^{\mathrm{T}}P_{m_3} + \frac{1}{2}q_3^2 + \frac{1}{2}\beta_{3,k}^2 \le \frac{1}{2}\ell_3^2 + \frac{1}{2\ell_3^2}q_3^2\lambda_3P_{m_3}^{\mathrm{T}}P_{m_3} + \frac{1}{2}q_3^2 + \frac{1}{2}\beta_{3,k}^2 \tag{39}$$

where $\ell_3 > 0$ is a constant.

Then, the intermediate control signal ξ_3 is designed as follows

$$\xi_3 = -\left(w_3 + \frac{1}{2}\right)q_3 - \frac{1}{2\ell_3^2}q_3\,\hat{\lambda}_3P_{m_3}^{\mathrm{T}}P_{m_3} \tag{40}$$

where $w_3 > 0$ is a constant.

Combining (31), (37), (39) and (40), one has

$$\dot{\Psi}_3 \le -\sum_{j=1}^{3}c_jq_j^2 + \frac{1}{2}q_4^2 + [\kappa(t)N(\varsigma)+1]\,\dot{\varsigma} + \frac{1}{2}\sum_{j=1}^{3}\ell_j^2 + \frac{1}{2}\sum_{j=1}^{3}\beta_{j,k}^2 + \sum_{j=1}^{3}a_j^2 + \frac{1}{2}a_2^2 + \sum_{j=1}^{3}\tilde{\lambda}_j\left(\frac{1}{2\ell_j^2}q_j^2P_{m_j}^{\mathrm{T}}P_{m_j} - \dot{\hat{\lambda}}_j\right) \tag{41}$$

Step $i\,(4 \le i \le n-1)$: The candidate Lyapunov functions are considered as follows

$$\Psi_i = \Psi_{i-1} + \frac{1}{2}q_i^2 + \frac{1}{2}\tilde{\lambda}_i^2 \tag{42}$$

The time derivative of the above Lyapunov functions Ψ_i can be represented as

$$\dot{\Psi}_i = q_i\left(q_{i+1} + \xi_i + h_{i,k}\left(\bar{\boldsymbol{\phi}}_i\right) + \Delta_{i,k}\left(t, \bar{\boldsymbol{\phi}}_i\right)\right) - q_i\dot{\xi}_{i-1} - \tilde{\lambda}_i\dot{\hat{\lambda}}_i + \dot{\Psi}_{i-1} \tag{43}$$

where

$$\dot{\xi}_{i-1} = \frac{\partial \xi_{i-1}}{\partial y}\dot{y} + \sum_{j=0}^{i-1}\frac{\partial \xi_{i-1}}{\partial y_d^{(j)}}y_d^{(j+1)} + \sum_{j=1}^{i-1}\frac{\partial \xi_{i-1}}{\partial \phi_j}\dot{\phi}_j + \frac{\partial \xi_{i-1}}{\partial \varsigma}\dot{\varsigma} + \sum_{j=1}^{i-1}\frac{\partial \xi_{i-1}}{\partial \hat{\lambda}_j}\dot{\hat{\lambda}}_j.$$

According to Young's inequality, the following inequalities can be obtained.

$$\begin{aligned}-q_i\dot{\xi}_{i-1} \le\ & \frac{1}{a_{i-1}^2}q_i^2\left(\frac{\partial \xi_{i-1}}{\partial y}\right)^2\bar{\kappa}^2\left(\phi_2+\gamma_{1,k}\right)^2 \\ & - q_i\sum_{j=0}^{i-1}\frac{\partial \xi_{i-1}}{\partial y_d^{(j)}}y_d^{(j+1)} - q_i\sum_{j=1}^{i-1}\frac{\partial \xi_{i-1}}{\partial \hat{\lambda}_j}\dot{\hat{\lambda}}_j \\ & + \frac{1}{a_{i-1}^2}q_i^2\sum_{j=1}^{i-1}\left(\frac{\partial \xi_{i-1}}{\partial \phi_j}\right)^2\left(\phi_{j+1}+\gamma_{j,k}\right)^2 \\ & + \frac{1}{2}a_{i-1}^2 - q_i\frac{\partial \xi_{i-1}}{\partial \varsigma}\dot{\varsigma}\end{aligned} \tag{44}$$

$$q_iq_{i+1} \le \frac{1}{2}q_i^2 + \frac{1}{2}q_{i+1}^2 \tag{45}$$

$$q_i\left(h_{i,k}\left(\bar{\boldsymbol{\phi}}_i\right) + \Delta_{i,k}\left(t, \bar{\boldsymbol{\phi}}_i\right)\right) \le a_i^2 + \frac{1}{4a_i^2}q_i^2\gamma_{i,k}^2 \tag{46}$$

with $\gamma_{i,k} = h_{i,k}(\bar{\boldsymbol{\phi}}_i) + \varphi_{i,k}(t, \bar{\boldsymbol{\phi}}_i) + \tilde{\varphi}_{i,k}$, and $a_i > 0$ are constants.

Substituting (44), (45) and (46) into (43), the following inequality holds

$$\dot{\Psi}_i \le \dot{\Psi}_{i-1} + \frac{1}{2}q_i^2 + \frac{1}{2}q_{i+1}^2 + q_i\xi_i + a_i^2 + \frac{1}{2}a_{i-1}^2 + q_i\mathrm{H}_{i,k} - \frac{1}{2}q_i^2 - \tilde{\lambda}_i\dot{\hat{\lambda}}_i \tag{47}$$

where

$$\begin{aligned}\mathrm{H}_{i,k} =\ & \frac{1}{4a_i^2}q_i\gamma_{i,k}^2 + \frac{1}{a_{i-1}^2}q_i\left(\frac{\partial \xi_{i-1}}{\partial y}\right)^2\bar{\kappa}^2(\phi_2+\gamma_{1,k})^2 \\ & - \sum_{j=0}^{i-1}\frac{\partial \xi_{i-1}}{\partial y_d^{(j)}}y_d^{(j+1)} - \frac{\partial \xi_{i-1}}{\partial \varsigma}\dot{\varsigma} + \frac{1}{2}q_i \\ & - \sum_{j=1}^{i-1}\frac{\partial \xi_{i-1}}{\partial \hat{\lambda}_j}\dot{\hat{\lambda}}_j + \frac{1}{a_{i-1}^2}q_i\sum_{j=1}^{i-1}\left(\frac{\partial \xi_{i-1}}{\partial \phi_j}\right)^2(\phi_{j+1}+\gamma_{j,k})^2.\end{aligned}$$

According to Lemma 2.2, for $\forall\beta_{i,k} > 0$, exist an MTN that can be used to approximate $\mathrm{H}_{i,k}$, such as

$$\mathrm{H}_{i,k} = \boldsymbol{\lambda}_{i,k}^{\mathrm{T}}P_{m_i} + \delta_{i,k}\left(\boldsymbol{q}_i\right), \left|\delta_{i,k}\left(\boldsymbol{q}_i\right)\right| \le \beta_{i,k} \tag{48}$$

with $\boldsymbol{q}_i = [q_1, q_2, \ldots, q_i]^{\mathrm{T}}$. $\delta_{i,k}(\boldsymbol{q}_i)$ are the error between $\mathrm{H}_{i,k}$ and $\boldsymbol{\lambda}_{i,k}^{\mathrm{T}}P_{m_i}$.

With the help of Young's inequality and taking (48) into account, the following inequality holds

$$\begin{aligned}q_i\mathrm{H}_{i,k} &= q_i\boldsymbol{\lambda}_{i,k}^{\mathrm{T}}P_{m_i} + q_i\delta_{i,k} \\ &\le \frac{1}{2}\ell_i^2 + \frac{1}{2\ell_i^2}q_i^2\left\|\boldsymbol{\lambda}_{i,k}\right\|^2P_{m_i}^{\mathrm{T}}P_{m_i} + \frac{1}{2}q_i^2 + \frac{1}{2}\beta_{i,k}^2 \\ &\le \frac{1}{2}\ell_i^2 + \frac{1}{2\ell_i^2}q_i^2\lambda_iP_{m_i}^{\mathrm{T}}P_{m_i} + \frac{1}{2}q_i^2 + \frac{1}{2}\beta_{i,k}^2\end{aligned} \tag{49}$$

where $\ell_i > 0$ are constants.

Then, the intermediate control signals ξ_i are designed as follows

$$\xi_i = -\left(w_i + \frac{1}{2}\right)q_i - \frac{1}{2\ell_i^2}q_i\hat{\lambda}_iP_{m_i}^{\mathrm{T}}P_{m_i} \tag{50}$$

where $w_i > 0$ are constants.

Repeating *Step 3* and combining (47), (49), (50), one has

$$\begin{aligned}\dot{\Psi}_i \le\ & -\sum_{j=1}^{i}c_jq_j^2 + \frac{1}{2}q_{i+1}^2 + \left[\kappa(t)N(\varsigma)+1\right]\dot{\varsigma} \\ & + \sum_{j=1}^{i}\tilde{\lambda}_j\left(\frac{1}{2\ell_j^2}q_j^2P_{m_j}^{\mathrm{T}}P_{m_j} - \dot{\hat{\lambda}}_j\right) \\ & + \frac{1}{2}\sum_{j=1}^{i}\ell_j^2 + \frac{1}{2}\sum_{j=1}^{i}\beta_{j,k}^2 + \sum_{j=1}^{i}a_j^2 + \frac{1}{2}\sum_{j=2}^{i-1}a_j^2\end{aligned} \tag{51}$$

Remark 3.2: Term $\frac{1}{2}q_i^2, i = 3, 4, \ldots, n$ will be solved in the *Step i*.

Step n : The candidate Lyapunov function is considered as follows

$$\Psi_n = \Psi_{n-1} + \frac{1}{2}q_n^2 + \frac{1}{2}\tilde{\lambda}_n^2 \tag{52}$$

The time derivative of Ψ_n can be described as

$$\dot{\Psi}_n = q_n\left(u + h_{n,k}\left(\bar{\boldsymbol{\phi}}_n\right) + \Delta_{n,k}\left(t, \bar{\boldsymbol{\phi}}_n\right)\right) - q_n\dot{\xi}_{n-1} - \tilde{\lambda}_n\dot{\hat{\lambda}}_n + \dot{\Psi}_{n-1} \tag{53}$$

where

$$\dot{\xi}_{n-1} = \frac{\partial \xi_{n-1}}{\partial y}\dot{y} + \sum_{j=0}^{n-1}\frac{\partial \xi_{n-1}}{\partial y_d^{(j)}}y_d^{(j+1)} + \sum_{j=1}^{n-1}\frac{\partial \xi_{n-1}}{\partial \phi_j}\dot{\phi}_j + \frac{\partial \xi_{n-1}}{\partial \varsigma}\dot{\varsigma} + \sum_{j=1}^{n-1}\frac{\partial \xi_{n-1}}{\partial \hat{\lambda}_j}\dot{\hat{\lambda}}_j.$$

According to Young's inequality, the following inequalities can be obtained.

$$
\begin{aligned}
- q_n\dot{\xi}_{n-1} \le{}& \frac{1}{a_{n-1}^2} q_n^2 \left(\frac{\partial \xi_{n-1}}{\partial y}\right)^2 \bar{\kappa}^2 \left(\phi_2 + \gamma_{1,k}\right)^2 \\
&+ \frac{1}{2} a_{n-1}^2 + \frac{1}{a_{n-1}^2} q_n^2 \sum_{j=1}^{n-1} \left(\frac{\partial \xi_{n-1}}{\partial \phi_j}\right)^2 \left(\phi_{j+1} + \gamma_{j,k}\right)^2 \\
&- q_n \left(\sum_{j=0}^{n-1} \frac{\partial \xi_{n-1}}{\partial y_d^{(j)}} y_d^{(j+1)} + \frac{\partial \xi_{n-1}}{\partial \varsigma} \dot{\varsigma} + \sum_{j=1}^{n-1} \frac{\partial \xi_{n-1}}{\partial \hat{\lambda}_j} \dot{\hat{\lambda}}_j \right)
\end{aligned} \tag{54}
$$

$$
q_n \left(h_{n,k}\left(\bar{\boldsymbol{\phi}}_n\right) + \Delta_{n,k}\left(t, \bar{\boldsymbol{\phi}}_n\right) \right) \le a_n^2 + \frac{1}{4a_n^2} q_n^2 \gamma_{n,k}^2 \tag{55}
$$

with $\gamma_{n,k} = h_{n,k}(\bar{\boldsymbol{\phi}}_n) + \varphi_{n,k}(t, \bar{\boldsymbol{\phi}}_n) + \tilde{\varphi}_{n,k}$, and $a_n > 0$ is a constant.

Substituting (54) and (55) into (53), the following inequality holds

$$
\dot{\Psi}_n \le \dot{\Psi}_{n-1} + q_n u + a_n^2 + \frac{1}{2} a_{n-1}^2 + q_n \mathrm{H}_{n,k} - \tilde{\lambda}_n \dot{\hat{\lambda}}_n \tag{56}
$$

where

$$
\begin{aligned}
\mathrm{H}_{n,k} ={}& \frac{1}{4a_n^2} q_n \gamma_{n,k}^2 + \frac{1}{a_{n-1}^2} q_n \left(\frac{\partial \xi_{n-1}}{\partial y}\right)^2 \bar{\kappa}^2 (\phi_2 + \gamma_{1,k})^2 \\
&- \sum_{j=0}^{n-1} \frac{\partial \xi_{n-1}}{\partial y_d^{(j)}} y_d^{(j+1)} - \frac{\partial \xi_{n-1}}{\partial \varsigma} \dot{\varsigma} - \sum_{j=1}^{n-1} \frac{\partial \xi_{n-1}}{\partial \hat{\lambda}_j} \dot{\hat{\lambda}}_j \\
&+ \frac{1}{a_{n-1}^2} q_n \sum_{j=1}^{n-1} \left(\frac{\partial \xi_{n-1}}{\partial \phi_j}\right)^2 (\phi_{j+1} + \gamma_{j,k})^2.
\end{aligned}
$$

According to Lemma 2.2, for $\forall \beta_{n,k} > 0$, exist an MTN that can be used to approximate $\mathrm{H}_{n,k}$, such as

$$
\mathrm{H}_{n,k} = \boldsymbol{\lambda}_{n,k}^{\mathrm{T}} P_{m_n} + \delta_{n,k}\left(\boldsymbol{q}_n\right), \left|\delta_{n,k}\left(\boldsymbol{q}_n\right)\right| \le \beta_{n,k} \tag{57}
$$

with $\boldsymbol{q}_n = [q_1, q_2, \ldots, q_n]^{\mathrm{T}}$. $\delta_{n,k}(\boldsymbol{q}_n)$ is the error between $\mathrm{H}_{n,k}$ and $\lambda_{n,k}^{\mathrm{T}} P_{m_n}$.

From (57) and Young's inequality, the following inequality holds

$$
\begin{aligned}
q_n \mathrm{H}_{n,k} &= q_n \boldsymbol{\lambda}_{n,k}^{\mathrm{T}} P_{m_n} + q_n \delta_{n,k} \\
&\le \frac{1}{2} \ell_n^2 + \frac{1}{2\ell_n^2} q_n^2 \left\| \lambda_{n,k} \right\|^2 P_{m_n}^{\mathrm{T}} P_{m_n} + \frac{1}{2} q_n^2 + \frac{1}{2} \beta_{n,k}^2 \\
&\le \frac{1}{2} \ell_n^2 + \frac{1}{2\ell_n^2} q_n^2 \lambda_n P_{m_n}^{\mathrm{T}} P_{m_n} + \frac{1}{2} q_n^2 + \frac{1}{2} \beta_{n,k}^2
\end{aligned} \tag{58}
$$

where $\ell_n > 0$ is a constant.

Then, the control signal u is designed as follows

$$
u = -\left(w_n + \frac{1}{2}\right) q_n - \frac{1}{2\ell_n^2} q_n \hat{\lambda}_n P_{m_n}^{\mathrm{T}} P_{m_n} \tag{59}
$$

where $w_n > 0$ is a constant.

Combining (51), (56), (58) and (59), one has

$$
\begin{aligned}
\dot{\Psi}_n \le{}& - \sum_{j=1}^{n} c_j q_j^2 + \left[\kappa(t) N(\varsigma) + 1\right] \dot{\varsigma} + \frac{1}{2} \sum_{j=1}^{n} \ell_j^2 + \frac{1}{2} \sum_{j=1}^{n} \beta_{j,k}^2 \\
&+ \sum_{j=1}^{n} a_j^2 + \frac{1}{2} \sum_{j=2}^{n-1} a_j^2 + \sum_{j=1}^{n} \tilde{\lambda}_j \left(\frac{1}{2\ell_j^2} q_j^2 P_{m_j}^{\mathrm{T}} P_{m_j} - \dot{\hat{\lambda}}_j \right)
\end{aligned} \tag{60}
$$

4. Stability analysis

Theorem 4.1: *Switched nonlinear systems subject to unknown output hysteresis (1) is considered, if the virtual control signals and actual input control signal are devised as (20), (30), (40), (50) and (59), adaptive control laws are designed as*

$$
\dot{\hat{\lambda}}_j = -\eta_j \hat{\lambda}_j + \frac{1}{2\ell_j^2} q_j^2 P_{m_j}^{\mathrm{T}} P_{m_j} \tag{61}
$$

where $j = 1, 2, \ldots, n$, $\eta_j > 0$ are constants. For any bounded initial conditions, one has

(1) *For the closed-loop system, all signals in it are bounded.*
(2) *Tracking error, i.e. $y - y_d$, can converge to an adjustable region of the origin.*

Proof: The Lyapunov function is considered as follows

$$
\Psi = \Psi_n = \frac{1}{2} \sum_{j=1}^{n} q_j^2 + \frac{1}{2} \sum_{j=1}^{n} \tilde{\lambda}_j^2 \tag{62}
$$

According to (60), one has

$$
\begin{aligned}
\dot{\Psi} \le{}& - \sum_{j=1}^{n} c_j q_j^2 + \left[\kappa(t) N(\varsigma) + 1\right] \dot{\varsigma} + \frac{1}{2} \sum_{j=1}^{n} \ell_j^2 + \frac{1}{2} \sum_{j=1}^{n} \beta_{j,k}^2 \\
&+ \sum_{j=1}^{n} a_j^2 + \frac{1}{2} \sum_{j=2}^{n-1} a_j^2 + \sum_{j=1}^{n} \tilde{\lambda}_j \left(\frac{1}{2\ell_j^2} q_j^2 P_{m_j}^{\mathrm{T}} P_{m_j} - \dot{\hat{\lambda}}_j \right)
\end{aligned} \tag{63}
$$

Combining (61), $\tilde{\lambda}_j(\frac{1}{2\ell_j^2} q_j^2 P_{m_j}^{\mathrm{T}} P_{m_j} - \dot{\hat{\lambda}}_j)$ can be rewritten as

$$
\tilde{\lambda}_j \left(\frac{1}{2\ell_j^2} q_j^2 P_{m_j}^{\mathrm{T}} P_{m_j} - \dot{\hat{\lambda}}_j \right) \le -\frac{1}{2} \bar{\eta}_j \tilde{\lambda}_j^2 + \frac{1}{2} \eta_j \lambda_j^2 \tag{64}
$$

where $\bar{\eta}_j = \min\{\eta_j \mid j = 1, 2, \ldots, n\}$.

Substituting (64) into (63), the following inequality holds

$$
\dot{\Psi} \le a\Psi + b + \left[\kappa(t) N(\varsigma) + 1\right] \dot{\varsigma} \tag{65}
$$

where $a = \min\{2c_j, \bar{\eta}_j \mid j=1, 2, \ldots, n\}$, $\beta_{j,\max}^2 = \max\{\beta_{j,k}^2 \mid k \in M\}$, $b = \frac{1}{2} \sum_{j=1}^{n} \eta_j \lambda_j^2 + \frac{1}{2} \sum_{j=1}^{n} \ell_j^2 + \frac{1}{2} \sum_{j=1}^{n} \beta_{j,\max}^2 + \frac{3}{2} \sum_{j=1}^{n} a_j^2$.

Integrating (65), for $\forall t \geq 0$, the following inequality holds

$$0 \leq \Psi \leq \left[\Psi(0) - \frac{b}{a}\right] e^{-at} + \frac{b}{a} + e^{-at}\int_0^{\mathrm{T}} \left[\kappa(t) N(\varsigma) + 1\right] \dot{\varsigma} e^{a\tau}\, \mathrm{d}\tau \tag{66}$$

Based on inequality (66), using the method in Ma et al. (2019), it can be concluded that all signals in it are bounded, and the tracking error converges to a small region of the origin by designing appropriate parameters.

That completes the proof of Theorem 4.1. ■

5. Simulation study

To verify the effectiveness of the proposed controller, two examples are given in this section.

Example 5.1: The following switched nonlinear systems with the output hysteresis is discussed.

$$\begin{cases} \dot{\phi}_1 &= \phi_2 + h_{1,\sigma(t)}\left(\bar{\boldsymbol{\phi}}_1\right) + \Delta_{1,\sigma(t)}\left(t, \bar{\boldsymbol{\phi}}_1\right) \\ \dot{\phi}_2 &= \phi_3 + h_{2,\sigma(t)}\left(\bar{\boldsymbol{\phi}}_2\right) + \Delta_{2,\sigma(t)}\left(t, \bar{\boldsymbol{\phi}}_2\right) \\ \dot{\phi}_3 &= u + h_{3,\sigma(t)}\left(\bar{\boldsymbol{\phi}}_3\right) + \Delta_{3,\sigma(t)}\left(t, \bar{\boldsymbol{\phi}}_3\right) \\ y &= \rho_1\phi_1 + \rho_2\hbar \end{cases} \tag{67}$$

with initial states $\phi_1(0) = 0, \phi_2(0) = 0, \phi_3(0) = 0.$ $\sigma(t) : [0, \infty) \to M = \{1, 2\}$ is the switching signal. When $\sigma(t) = 1$, the nonlinear functions in the system are set as $h_{1,1} = -\frac{\phi_1^2 \sin\phi_1}{1+\phi_1^2}$, $h_{2,1} = -\frac{\phi_1^2 \sin(1+\phi_1^2)+1+\phi_2^2}{1+2\phi_1^2+3\phi_2^2}$, $h_{3,1} = -\frac{\sin\phi_3+2\phi_2^2+3\phi_3^2}{1+2\phi_1^2+3\phi_2^2+4\phi_3^2}$. The time-varying disturbance are set as $\Delta_{1,1} = -0.2x_1^2\sin(\frac{1}{1+\phi_1^2})$, $\Delta_{2,1} = -0.3\phi_2^2\sin\pi t$, $\Delta_{3,1} = 0.4\phi_3^2\sin\pi t$. When $\sigma(t) = 2$, the nonlinear functions in the system are set as $h_{1,2} = -\frac{\phi_1^2\cos\phi_1}{1+\phi_1^2}$, $h_{2,2} = -\frac{\phi_1^2\cos(1+\phi_1^2)+1+\phi_2^2}{1+2\phi_1^2+3\phi_2^2}$, $h_{3,2} = -\frac{\cos\phi_2+2\phi_2^2+3\phi_3^2}{1+2\phi_1^2+3\phi_2^2+4\phi_3^2}$. The time-varying disturbance are set as $\Delta_{1,2} = -0.2\phi_1^2\cos(\frac{1}{1+\phi_1^2})$, $\Delta_{2,2} = -0.3\phi_2^2\cos\pi t$, $\Delta_{3,2} = 0.4\phi_3^2\sin\pi t$.

The parameters of output hysteresis are set as follows: $\rho_1 = \rho_2 = 1, \iota = 5, K = 2, \varpi = 3.5$. Therefore, the output hysteresis can be expressed as $y = \phi_1 + \hbar$, with

$$\begin{cases} \dot{\hbar} &= \dot{\phi}_1 - 5|\dot{\phi}_1||\hbar|\hbar - 3.5\dot{\phi}_1|\hbar|^2 \\ \hbar_0 &= 0 \end{cases}.$$

According to Theorem 4.1, the control structure of systems (67) can be designed as follows

$$\begin{aligned} \xi_1 &= N(\varsigma)\left[\left(w_1 + \frac{1}{2}\right) q_1 + \frac{1}{2\ell_1^2} q_1 \hat{\lambda}_1 P_{m_1}^{\mathrm{T}} P_{m_1}\right] \\ \xi_2 &= -\left(w_2 + \frac{1}{2}\right) q_2 - \frac{1}{2\ell_2^2} q_2 \hat{\lambda}_2 P_{m_2}^{\mathrm{T}} P_{m_2} \\ u &= -\left(w_3 + \frac{1}{2}\right) q_3 - \frac{1}{2\ell_3^2} q_3 \hat{\lambda}_3 P_{m_3}^{\mathrm{T}} P_{m_3} \\ \dot{\hat{\lambda}}_j &= -\eta_j \hat{\lambda}_j + \frac{1}{2\ell_j^2} q_j^2 P_{m_j}^{\mathrm{T}} P_{m_j},\ j = 1, 2, 3 \end{aligned} \tag{68}$$

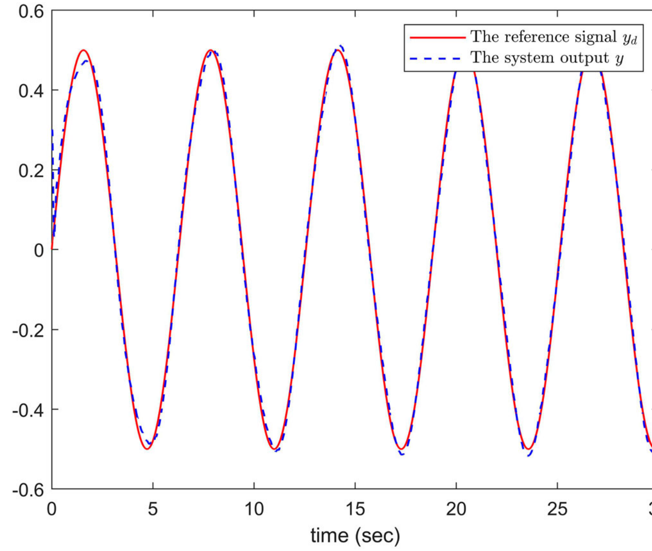

Figure 2. System output $y(t)$ and reference signal $y_d(t)$ of Example 5.1.

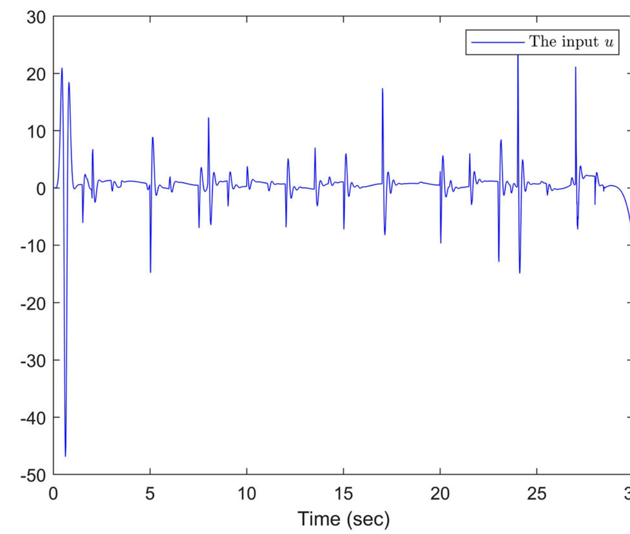

Figure 3. System control input of Example 5.1.

with $N(\varsigma) = \varsigma^2\cos\varsigma$, $\dot{\varsigma} = (w_1 + \frac{1}{2})q_1^2 + \frac{1}{2\ell_1^2} q_1^2 \hat{\lambda}_1 P_{m_1}^{\mathrm{T}} P_{m_1}$, $q_1 = \phi_1 - y_d$, $q_2 = \phi_2 - \xi_1$, $q_3 = \phi_3 - \xi_2$, $\boldsymbol{q}_1 = [q_1]^{\mathrm{T}}$, $\boldsymbol{q}_2 = [q_1, q_2]^{\mathrm{T}}$, $\boldsymbol{q}_3 = [q_1, q_2, q_3]^{\mathrm{T}}$. The parameters of the design controller are as follows: $w_1 = 29.5, w_2 = 19.5, w_3 = 79.5$, $\eta_1 = 2, \eta_2 = 1, \eta_3 = 0.2$, $\ell_1 = \ell_2 = \ell_3 = 1$. The simulation results are shown in Figures 2–6.

The output hysteresis $y(t)$ of systems and its reference signal $y_d(t)$ are given in Figure 2. Figures 3–5 reveal the trajectory of control input u, two state variables $\phi_2(t), \phi_3(t)$ and the switching signal $\sigma(t)$ of systems (67). In the light of the system output and its reference signal, the tracking error of systems is correlated in Figure 6. The tracking error converges in a small range of the origin. It can be seen from Figures 2–6 that satisfactory tracking effect can be attained by the controller proposed in this article.

Example 5.2: The electromechanical systems are used to verify the effectiveness of the proposed control strategy, which can be

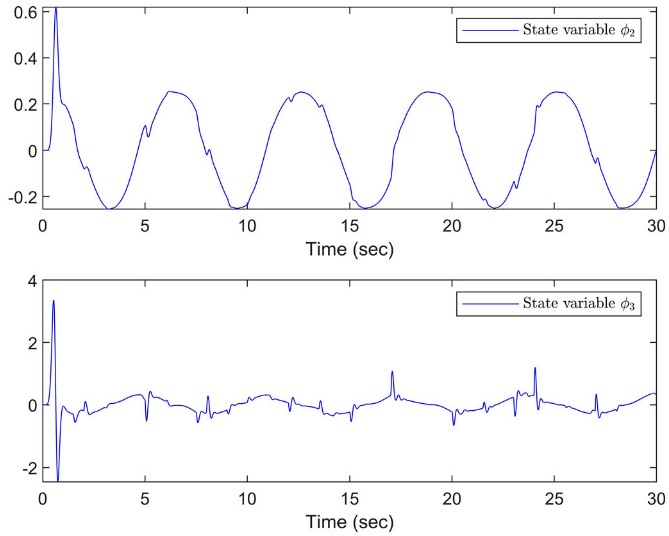

Figure 4. State variables ϕ_2, ϕ_3 of Example 5.1.

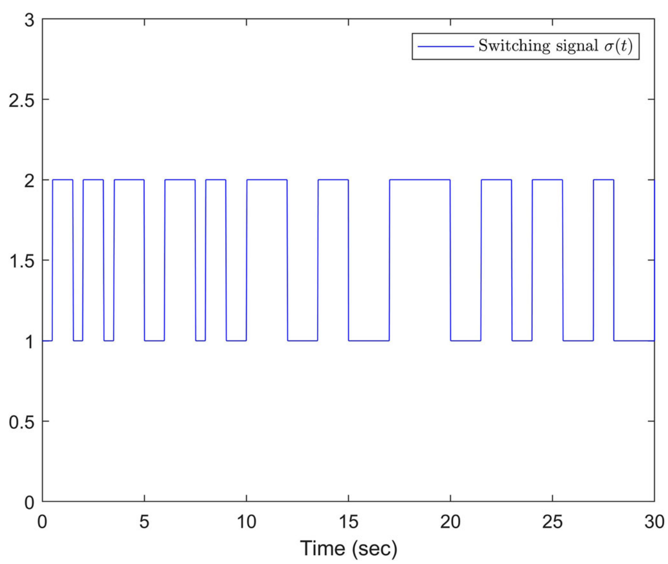

Figure 5. Switching signal of Example 5.1.

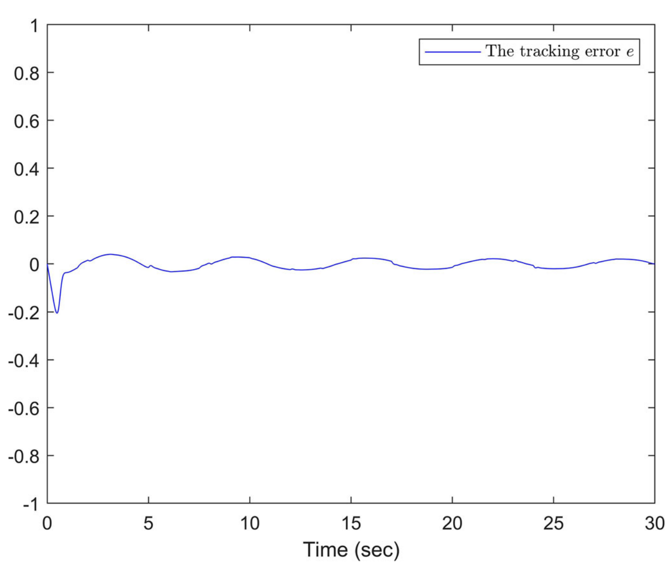

Figure 6. The tracking error of Example 5.1.

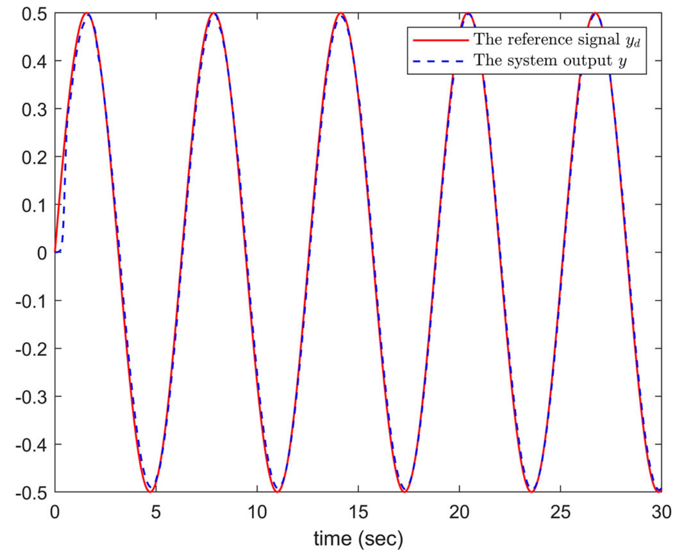

Figure 7. System output $y(t)$ and reference signal $y_d(t)$ of Example 5.2.

transformed as switched nonlinear systems (Lyu et al., 2019).

$$\begin{cases} \dot{\phi}_1 &= \phi_2 + h_{1,\sigma(t)}\left(\bar{\boldsymbol{\phi}}_1\right) + \Delta_{1,\sigma(t)}\left(t, \bar{\boldsymbol{\phi}}_1\right) \\ \dot{\phi}_2 &= \phi_3 + h_{2,\sigma(t)}\left(\bar{\boldsymbol{\phi}}_2\right) + \Delta_{2,\sigma(t)}\left(t, \bar{\boldsymbol{\phi}}_2\right) \\ \dot{\phi}_3 &= u + h_{3,\sigma(t)}\left(\bar{\boldsymbol{\phi}}_3\right) + \Delta_{3,\sigma(t)}\left(t, \bar{\boldsymbol{\phi}}_3\right) \\ y &= \rho_1\phi_1 + \rho_2\hbar \end{cases} \tag{69}$$

with the initial state, switching signal, the parameter settings of output hysteresis and the control structure of systems are the same as those in example 1. Among them, $h_{1,1} = h_{1,2} = 0$, $h_{2,1} = h_{2,2} = -\frac{N}{M}\sin\phi_1 - \frac{B}{M}\phi_2$, $h_{3,1} = -\frac{K_B}{ML}\phi_2 - \frac{R_2+R_3}{ML}\phi_3$, $h_{3,2} = -\frac{K_B}{ML}\phi_2 - \frac{R_1+R_3}{ML}\phi_3$ are the nonlinear functions. $\Delta_{1,1} = -0.1\phi_1 \sin t$, $\Delta_{1,2} = -0.3\phi_1 \cos t$, $\Delta_{2,1} = -0.2\phi_2 + \sin t$, $\Delta_{2,2} = -0.2\phi_2 + \cos t$, $\Delta_{3,1} = 0.3\phi_2 \sin \pi t$, $\Delta_{3,2} = 0.1\phi_2 \sin \pi t$ are the time-varying disturbances. The parameters design of electromechanical systems are $R_0 = 0.023$, $R_1 = 5$, $R_2 = 10$, $R_3 = 5$, $L_0 = 0.305$, $L = 15$, $m = 0.506$, $M_0 = 0.434$, $G = 9.8$, $B_0 = 1.625 \times 10^{-2}$, $J = 0.1625$, $K_r = K_B = 0.9$, $B = \frac{B_0}{K_r}$, $N = \frac{mL_0G}{2K_r} + \frac{M_0L_0G}{K_r}$, $M = \frac{J}{K_r} + \frac{mL_0^2}{3K_r} + \frac{M_0L_0^2}{K_r} + \frac{2M_0R_0^2}{5K_r}$.

Figures 7–11 show that the control strategy proposed in this article can still achieve good results for practical application systems. The above results further prove effectiveness of the proposed controller.

Remark 5.1: It can be seen from the Examples 5.1–5.2 that the superior tracking performance are acquired by choosing the optimal parameters. In theory, for switched nonlinear systems (1), based on Theorem 4.1, it can be concluded that the tracking performance can be achieved when η_i, w_i, ℓ_i are positive constants. However, in practice, in order to obtain the specific control objective, it is necessary to obtain optimal tracking performance by continuously adjusting design parameters.

Remark 5.2: For the system (67) with the initial states $\boldsymbol{\phi}(\mathbf{0}) = [0.3, 0, 0]^{\mathrm{T}}$, the tracking control performance and control input are displayed in Figure 12. It can be clearly seen that the control

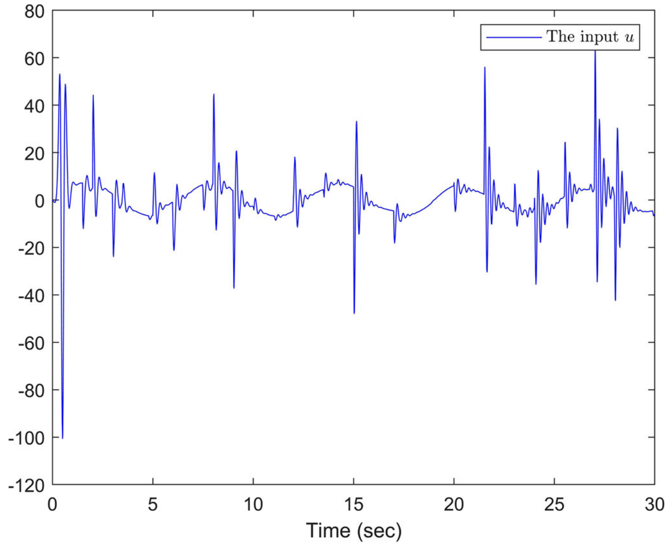

Figure 8. System control input of Example 5.2.

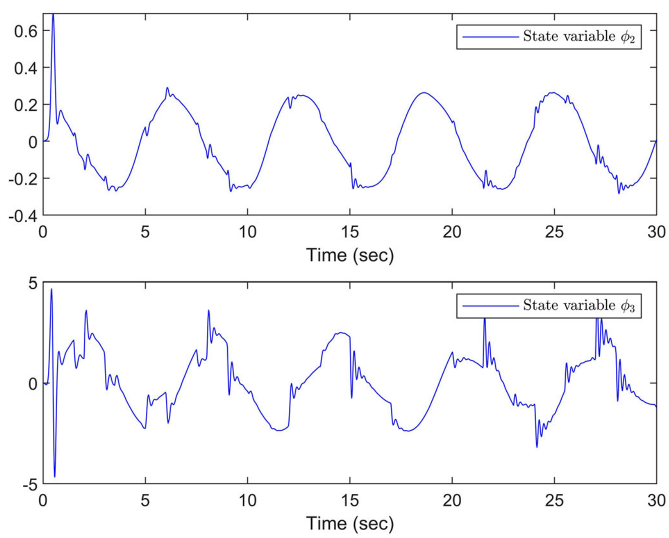

Figure 9. State variables ϕ_2, ϕ_3 of Example 5.2.

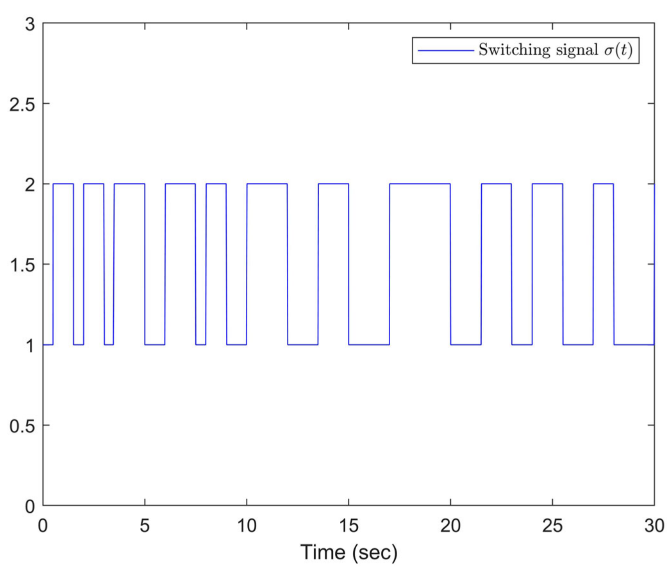

Figure 10. Switching signal of Example 5.2.

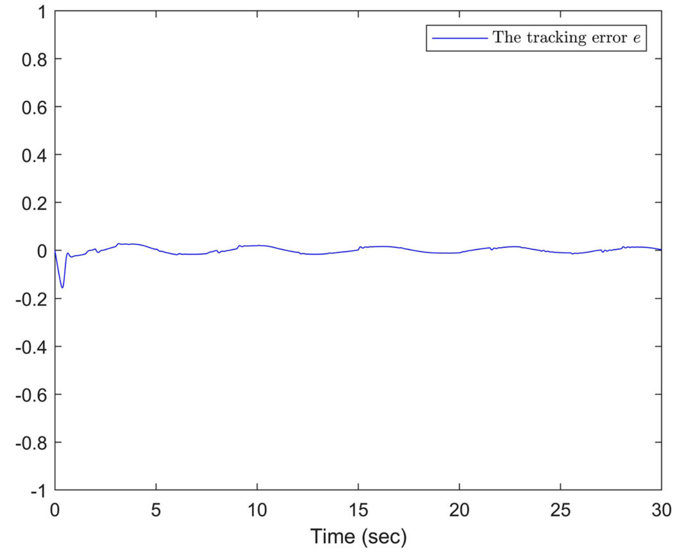

Figure 11. The tracking error of Example 5.2.

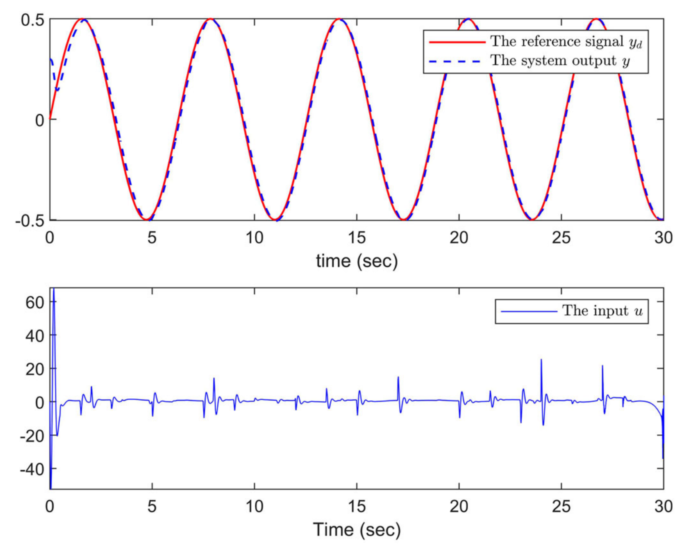

Figure 12. The tracking control performance of system (67) with the initial states $\boldsymbol{\phi}(\mathbf{0}) = [0.3, 0, 0]^{\mathrm{T}}$.

effect is still satisfactory in the case of large error initialisation, and a large control input is required at the initial stage of control for the purpose of quickly acquiring superior tracking performance. It is concluded that the control strategy proposed in this article is able to achieve real-time tracking in a short period of time, and satisfactory results can still be acquired in the case of large error initialisation.

6. Conclusion

The tracking control problem of a class of switched nonlinear systems subject to output hysteresis is studied in this article. First, the nonlinearity of output hysteresis is transformed into the combination of a disturbance term and a linear term by using the modified Bouc–Wen hysteresis model. Then, an adaptive MTN control method is proposed based on backstepping technique. It should be pointed out that the adaptive

MTN method is extended to switched nonlinear systems subject to output hysteresis for the first time. The proposed control method simplifies the backstepping design process from two aspects. On the one hand, only one MTN is adopted to estimate the nonlinear functions that appear in each step of backstepping. On the other hand, the modified Bouc–Wen hysteresis model is introduced to solve the nonlinearity caused by output hysteresis. At the end, two simulation examples show that the proposed control strategy is effective.

The next research topic is to further consider the case of unmeasured state based on the research in this article and acquire a novel MTN-based adaptive control strategy. For tracking control of switched nonlinear systems subject to output hysteresis, it is a major challenge to construct a reasonable state observer and obtain a simple controller.

Disclosure statement

No potential conflict of interest was reported by the author(s).

Funding

This work was supported by the Shandong Provincial Natural Science Foundation, China [grant number ZR2020QF055].

ORCID

Wen-Jing He http://orcid.org/0000-0001-6370-592X
Shan-Liang Zhu http://orcid.org/0000-0002-6194-3614
Na Li http://orcid.org/0000-0002-7911-8903
Yu-Qun Han http://orcid.org/0000-0002-9055-2954

References

Cassandras, C. G., Pepyne, D. L., & Wardi, Y. (2001). Optimal control of a class of hybrid systems. *IEEE Transactions on Automatic Control*, *46*(3), 398–415. https://doi.org/10.1109/9.911417

Chen, X. K., Su, C. Y., & Fukuda, T. (2008). Adaptive control for the systems preceded by hysteresis. *IEEE Transactions on Automatic Control*, *53*(4), 1019–1025. https://doi.org/10.1109/TAC.2008.919551

Chiang, M. L., & Fu, L. C. (2014). Adaptive stabilization of a class of uncertain switched nonlinear systems with backstepping control. *Automatica*, *50*(8), 2128–2135. https://doi.org/10.1016/j.automatica.2014.05.029

Chu, L., Gao, T., Wang, M. X., Han, Y. Q., & Zhu, S. L. (2021). Adaptive decentralized control for large-scale nonlinear systems with finite-time output constraints by multi-dimensional Taylor network. *Asian Journal of Control*. https://doi.org/10.1002/asjc.2571

Duan, Z. Y., Yan, H. S., & Zheng, X. Y. (2020). Robust model predictive control based on recurrent multi-dimensional Taylor network for discrete-time non-linear time-delay systems. *IET Control Theory and Applications*, *14*(3), 1806–1818. https://doi.org/10.1049/cth2.v14.13

Gong, Z. H., Liu, C. Y., Feng, E. M., Wang, L., & Yu, Y. S. (2011). Modelling and optimization for a switched system in microbial fed-batch culture. *Applied Mathematical Modelling*, *35*(7), 3276–3284. https://doi.org/10.1016/j.apm.2011.01.023

Han, J. C., Hu, J., Yang, O. Y., Wang, S. X., & He, J. L. (2015). Hysteretic modeling of output characteristics of giant magnetoresistive current sensors. *IEEE Transactions on Industrial Electronics*, *62*(1), 516–524. https://doi.org/10.1109/TIE.2014.2326989

Han, Y. Q. (2018). Output-feedback adaptive tracking control of stochastic nonlinear systems using multi-dimensional Taylor network. *International Journal of Adaptive Control and Signal Processing*, *32*(3), 494–510. https://doi.org/10.1002/acs.v32.3

Han, Y. Q. (2021). Adaptive tracking control of a class of nonlinear systems with unknown dead-zone output: a multi-dimensional Taylor network (MTN)-based approach. *International Journal of Control*, *94*(11), 3161–3170. https://doi.org/10.1080/00207179.2020.1752941

Han, Y. Q., He, W. J., Li, N., & Zhu, S. L. (2021). Adaptive tracking control of a class of nonlinear systems with input delay and dynamic uncertainties using multi-dimensional Taylor network. *International Journal of Control, Automation and Systems*, *19*(12), 4078–4089. https://doi.org/10.1007/s12555-020-0708-y

Han, Y. Q., Li, N., He, W. J., & Zhu, S. L. (2021). Adaptive multi-dimensional Taylor network funnel control of a class of nonlinear systems with asymmetric input saturation. *International Journal of Adaptive Control and Signal Processing*, *35*(5), 713–726. https://doi.org/10.1002/acs.v35.5

He, W. J., Han, Y. Q., Li, N., & Zhu, S. L. (2022). Novel adaptive controller design for a class of switched nonlinear systems subject to input delay using multi-dimensional Taylor network. *International Journal of Adaptive Control and Signal Processing*, *36*(3), 607–624. https://doi.org/10.1002/acs.v36.3

Henzinger, T. A., Ho, P., & Wong-Toi, H. (1998). Algorithmic analysis of nonlinear hybrid systems. *IEEE Transactions on Automatic Control*, *43*(4), 540–554. https://doi.org/10.1109/9.664156

Juloski, A. L., Weiland, S., & Heemels, W. P. M. H. (2005). A Bayesian approach to identification of hybrid systems. *IEEE Transactions on Automatic Control*, *50*(10), 1520–1533. https://doi.org/10.1109/TAC.2005.856649

Lai, G. Y., Liu, Z., Zhang, Y., C. L. P. Chen, & Xie, S. L. (2018). Adaptive backstepping-based tracking control of a class of uncertain switched nonlinear systems. *Automatica*, *91*, 301–310. https://doi.org/10.1016/j.automatica.2017.12.008

Li, H. T., Peng, Y. F., & Wu, K. L. (2021). The existence and uniqueness of the solutions of the nonlinear on-off switched systems with switching at variable times. *Nonlinear Dynamics*, *103*(3), 2287–2298. https://doi.org/10.1007/s11071-021-06214-8

Li, S., Ahn, C. K., Chadli, M., & Xiang, Z. R. (2021). Sampled-data adaptive fuzzy control of switched large-scale nonlinear delay systems. *IEEE Transactions on Fuzzy Systems*, *30*(4), 1014–1024. https://doi.org/10.1109/TFUZZ.2021.3052094

Li, S., Ahn, C. K., & Xiang, Z. R. (2019a). Adaptive fuzzy control of switched nonlinear time-varying delay systems with prescribed performance and unmodeled dynamics. *Fuzzy Sets and Systems*, *371*, 40–60. https://doi.org/10.1016/j.fss.2018.10.011

Li, S., Ahn, C. K., & Xiang, Z. R. (2019b). Sampled-data adaptive output feedback fuzzy stabilization for switched nonlinear systems with asynchronous switching. *IEEE Transactions on Fuzzy Systems*, *27*(1), 200–205. https://doi.org/10.1109/TFUZZ.2018.2881660

Li, S., Ahn, C. K., & Xiang, Z. R. (2021). Command-filter-based adaptive fuzzy finite-time control for switched nonlinear systems using state-dependent switching method. *IEEE Transactions on Fuzzy Systems*, *29*(4), 833–845. https://doi.org/10.1109/TFUZZ.2020.2965917

Li, Y. M., Tong, S. C., & Li, T. S. (2014). Adaptive fuzzy output-feedback control for output constrained nonlinear systems in the presence of input saturation. *Fuzzy Sets and Systems*, *248*, 138–155. https://doi.org/10.1016/j.fss.2013.11.006

Liu, Z., Lai, G. Y., Zhang, Y., & Chen, C. L. P. (2015). Adaptive neural output feedback control of output-constrained nonlinear systems with unknown output nonlinearity. *IEEE Transactions on Neural Networks & Learning Systems*, *26*(8), 1789–1802. https://doi.org/10.1109/TNNLS.2014.2357036

Liu, Z. L., Chen, B., & Lin, C. (2017). Adaptive neural backstepping for a class of switched nonlinear system without strict-feedback form. *IEEE Transactions on Systems, Man, and Cybernetics: Systems*, *47*(7), 1315–1320. https://doi.org/10.1109/TSMC.2016.2585664

Lyu, Z. L., Liu, Z., Zhang, Y., & Chen, C. L. P. (2019). Adaptive neural control for switched nonlinear systems with unmodeled dynamics and unknown output hysteresis. *Neurocomputing*, *314*, 107–117. https://doi.org/10.1016/j.neucom.2019.02.057

Ma, L., Huo, X., Zhao, X. D., Niu, B., & Zong, G. D. (2019). Adaptive neural control for switched nonlinear systems with unknown backlash-like hysteresis and output dead-zone. *Neurocomputing*, *357*, 203–214. https://doi.org/10.1016/j.neucom.2019.04.049

Ma, R. C., & Zhao, J. (2010). Backstepping design for global stabilization of switched nonlinear systems in lower triangular form under arbitrary switchings. *Automatica*, *46*(11), 1819–1823. https://doi.org/10.1016/j.automatica.2010.06.050

Mao, J., Ahn, C. K., & Xiang, Z. R. (2022). Global stabilization for a class of switched nonlinear time-delay systems via sampled-data output-feedback control. *IEEE Transactions on Systems, Man, and Cybernetics: Systems*, *52*(2), 694–705. https://doi.org/10.1109/TSMC.2020.3048064

Min, C. Q., Dahlmann, M., & Sattel, T. (2021). Steady state response analysis for a switched stiffness vibration control system based on vibration energy conversion. *Nonlinear Dynamics*, *103*(1), 239–254. https://doi.org/10.1007/s11071-020-06147-8

Niu, B., Ahn, C. K., Li, H., & Liu, M. (2018). Adaptive control for stochastic switched nonlower triangular nonlinear systems and its application to a one-link manipulator. *IEEE Transactions on Systems, Man, and Cybernetics: Systems*, *48*(10), 1701–1714. https://doi.org/10.1109/TSMC.2017.2685638

Niu, B., & Li, L. (2018). Adaptive backstepping-based neural tracking control for MIMO nonlinear switched systems subject to input delays. *IEEE Transactions on Neural Networks and Learning Systems*, *29*(6), 2638–2644. https://doi.org/10.1109/TNNLS.2017.2690465

Niu, B., Liu, Y. J., Zhou, W. L., Li, H. T., Duan, P. Y., & Li, J. Q. (2020). Multiple Lyapunov functions for adaptive neural tracking control of switched nonlinear nonlower-triangular systems. *IEEE Transactions on Cybernetics*, *50*(5), 1877–1886. https://doi.org/10.1109/TCYB.2621036

Niu, B., & Zhao, J. (2012). Robust H∞ control for a class of switched nonlinear cascade systems via multiple Lyapunov functions approach. *Applied Mathematics and Computation*, *218*(11), 6330–6339. https://doi.org/10.1016/j.amc.2011.09.059

Su, C. Y., Stepanenko, Y., Svoboda, J., & Leung, T. P. (2000). Robust adaptive control of a class of nonlinear systems with unknown backlash-like hysteresis. *IEEE Transactions on Automatic Control*, *45*(12), 2427–2432. https://doi.org/10.1109/9.895588

Tao, G., & Kokotovic, P. V. (1995). Adaptive control of plants with unknown hystereses. *IEEE Transactions on Automatic Control*, *40*(2), 200–212. https://doi.org/10.1109/9.341778

Wu, C. Y., Li, J., Niu, B., & X. P. Huang (2020). Switched concurrent learning adaptive control of switched systems with nonlinear matched uncertainties. *IEEE Access*, *8*, 33560–33573. https://doi.org/10.1109/Access.6287639

Xiang, Z. R., Sun, Y. N., & Mahmoud, M. S. (2012). Robust finite-time H∞ control for a class of uncertain switched neutral systems. *Communications in Nonlinear Science and Numerical Simulation*, *17*(4), 1766–1778. https://doi.org/10.1016/j.cnsns.2011.09.022

Yan, H. S., & Duan, Z. Y. (2021). Tube-based model predictive control using multidimensional Taylor network for nonlinear time-delay systems. *IEEE Transactions on Automatic Control*, *66*(5), 2099–2114. https://doi.org/10.1109/TAC.2020.3005674

Yin, Q. T., Wang, M., & Jing, H. (2020). Stabilizing backstepping controller design for arbitrarily switched complex nonlinear system. *Applied Mathematics and Computation*, *369*, 124789. https://doi.org/10.1016/j.amc.2019.124789

Yue, F. F., & Li, X. F. (2019). Adaptive sliding mode control based on friction compensation for opto-electronic tracking system using neural network approximations. *Nonlinear Dynamics*, *96*(4), 2601–2612. https://doi.org/10.1007/s11071-019-04945-3

Zhang, J., Li, S., Ahn, C. K., & Xiang, Z. R. (2021). Adaptive fuzzy decentralized dynamic surface control for switched large-scale nonlinear systems with full-state constraints. *IEEE Transactions on Cybernetics*. https://doi.org/10.1109/TCYB.2021.3069461

Zhang, R., Wang, Y., Zhang, Z. D., & Bi, Q. S. (2015). Nonlinear behaviors as well as the bifurcation mechanism in switched dynamical systems. *Nonlinear Dynamics*, *79*(1), 465–471. https://doi.org/10.1007/s11071-014-1679-4

Zhang, T. P., & S. S. Ge (2007). Adaptive neural control of MIMO nonlinear state time-varying delay systems with unknown dead-zones and gain signs. *Automatica*, *43*(6), 1021–1033. https://doi.org/10.1016/j.automatica.2006.12.014

Zhao, F., Koutsoukos, X., Haussecker, H., Reich, J., & Cheung, P. (2005). Monitoring and fault diagnosis of hybrid systems. *IEEE Transactions on Systems, Man and Cybernetics, Part B (Cybernetics)*, *35*(6), 1225–1240. https://doi.org/10.1109/TSMCB.2005.850178

Zhou, J., Wen, C. Y., & Li, T. S. (2012). Adaptive output feedback control of uncertain nonlinear systems with hysteresis nonlinearity. *IEEE Transactions on Automatic Control*, *57*(10), 2627–2633. https://doi.org/10.1109/TAC.2012.2190208

Zhu, S. L., Duan, D. Y., Chu, L., Wang, M. X., Han, Y. Q., & P. C. Xiong (2020). Adaptive multi-dimensional Taylor network tracking control for a class of switched nonlinear systems with input nonlinearity. *Transactions of the Institute of Measurement and Control*, *42*(13), 2482–2491. https://doi.org/10.1177/0142331220916601

Zou, W. C., Ahn, C. K., & Xiang, Z. R. (2021). Fuzzy-approximation-based distributed fault-tolerant consensus for heterogeneous switched nonlinear multiagent systems. *IEEE Transactions on Fuzzy Systems*, *29*(10), 2916–2925. https://doi.org/10.1109/TFUZZ.2020.3009730